Absolute doubly differential cross sections for electron emission in collisions of 3.5-MeV/u Fe^{17+} and Fe^{22+} ions with He and Ar gas targets

D. H. Schneider, D. R. DeWitt, and R. W. Bauer
Lawrence Livermore National Laboratory, Livermore, California 94550

J. R. Mowat
North Carolina State University, Raleigh, North Carolina 29695

W. G. Graham
Queen's University, Belfast, Northern Ireland, United Kingdom

A. S. Schlachter
Lawrence Berkeley Laboratory, Berkeley, California 94720

B. Skogvall
Hahn-Meitner Institut, 1000 Berlin 39, Germany

P. Fainstein
Centro Atomico Bariloche and Instituto Balseiro, 8400 Bariloche, Argentina

R. D. Rivarola
Instituto de Fisica Rosario, Consejo Nacional de Investigaciones Científicas y Técnicas, and Universidad Nacional de Rosario, Rosario, Argentina

(Received 6 November 1990; revised manuscript received 27 March 1991)

Absolute doubly differential cross sections have been measured as a function of electron energy and angle of observation for electron emission in collisions of 3.5-MeV/u Fe^{17+} and Fe^{22+} ions with He and Ar gas targets under single-collision conditions. The measured electron emission cross sections are compared to theoretical and scaled cross sections based on the Born approximation. The results using intermediate-mass ions are discussed with reference to previously reported cross sections from collisions with highly charged lighter- and heavier-ion species at MeV/u projectile energies. The continuum–distorted-wave–eikonal-initial-state approximation shows good agreement with experiments except in the "binary-encounter peak" where the interaction between projectile electrons and target electrons could play an important role.

PACS number(s): 34.10.+x

INTRODUCTION

The present studies of the secondary-electron emission in collisions of 3.5-MeV/u Fe^{17+} and Fe^{22+} ions with He and Ar atoms are a continuation of recent investigations involving collisions of fast highly charged heavy ions (5 to 25-MeV/u C^{6+}, O^{8+}, Ne^{10+}, Mo^{40+}, Th^{38+}, and U^{38+}) with various gas targets [1]. The plane-wave born approximation (PWBA) was found to be in good agreement with the experimental data for fast *light*-ion impact on He and Ar targets [2–8]. In these cases the electron emission is basically determined by the potential of the target atom and the ionization is well described by the first Born approximation. For fast *heavy*-ion impact, however, it has been demonstrated that the doubly differential electron emission cross sections are not in good agreement with the PWBA; investigations of the electron emission probabilities for heavy-ion projectiles have been recognized to provide a sensitive measure of the dynamics of the ionization process during the collision [9–11]. It has been found that in fast collisions with highly charged projectiles, particularly at high electron emission energies, the contribution of higher-order effects can be studied. The existence of such effects, associated with the simultaneous presence of the projectile and target fields, is demonstrated through a comparison with experimental cross sections scaled according to the Born approximation and with other theories, e.g., the classical trajectory monte carlo (CTMC) calculations [12–14] and the continuum-distorted-wave–eikonal-initial-state (CDW-EIS) calculations [15,16].

It has been found that at forward and backward emission angles, for electrons emitted around 1 keV, there is a deviation between cross sections deduced from the scaled PWBA and experimental cross sections [11]. In the case of highly charged heavy ions the forces of both nuclei are important, so that the "single-center emission" concept breaks down and a "two-center emission" picture must be introduced for faster electrons. The higher-energy electrons sense more of the two potentials from the two

nuclei when departing from the collision [11]. This two-center emission concept was evaluated quantum mechanically in the CDW-EIS calculation and found to be in fair agreement with the experimental results obtained from 25-MeV/u Mo^{40+} collisions with He [11]. Good agreement between experiment and theory was also found by applying the CTMC codes to obtain doubly differential cross section for the previously investigated collision systems [10].

In this work we have chosen an intermediate projectile with nuclear change Z_p and two different charge states to extend our systematic study. The case of iron Fe^{17+} and Fe^{22+} as projectiles is of particular interest because of its relevance to plasma physics research (e.g., tokamak and astrophysical plasmas).

EXPERIMENTAL PROCEDURE

The doubly differential cross sections for electron emission between a few eV to about 8-keV electron energies, following collisions of 3.5-MeV/u Fe^{17+} and Fe^{22+} ions on He, Ar, and CH_4 atoms, have been determined absolutely for the observation angles ranging from 27° to 155°. The experiments have been performed at the SuperHILAC facility at the Lawrence Berkeley Laboratory.

The experimental setup has been described previously in Ref. [1]. It is similar to the setup developed at the Hahn-Meitner Institute in Berlin [10] including the experimental method given in earlier references (e.g., Ref. [4]). The tightly collimated ion beam interacts with the gas target maintained by a jet in the center of the magnetically shielded scattering chamber. The secondary-electron emission is observed at different observation angles using a 45° electrostatic parallel-plate analyzer rotatable in one plane around the scattering center.

The target density produced by the gas jet is about 10^{14} atoms/cm^3 over a target length of about 3 mm. This density ensures single-collision conditions. The analyzer has an energy resolution of about 9% full width at half maximum (FWHM) and a solid angle of 4×10^{-3} sr.

As described in Ref. [4] the actual target density is obtained by comparing electron yields measured from the gas target jet in place with those measured from a homogeneous target (with the jet removed). The channel plate detector used for electron detection has been calibrated with electron beams at different electron energies. As reported in Ref. [1] the Ar L Auger-electron emission has been used to cross check the absolute cross sections in comparison with the theoretical cross sections. The total L shell ionization cross section for 3.5-MeV/u Fe^{22+} on Ar was found to be 1.8×10^{-15} cm^2, which yields a total Ar L Auger-electron production cross section of 1.26×10^{-15} cm^2, if a mean L shell fluorescence yield of 30% is taken into account, which agrees within ±40% with the theoretical value.

The continuum electron spectra were corrected for background contributions from measurements without a gas target. For the doubly differential cross sections we estimated a relative uncertainty of about 30% and an absolute error of about 40%.

RESULTS AND DISCUSSIONS

Figures 1(a) and 1(b) and Figs. 2(a), 2(b), and 2(c) present a summary of the doubly differential cross sections for secondary-electron emission from 3.5-MeV/u Fe^{22+} on He and Ar, and 3.5-MeV/u Fe^{17+} on He, Ar, and CH_4, respectively. The cross sections display a maximum at electron energies of about 10 eV and fall off by several orders of magnitude towards the high-energy limit of the measurement at electrons energies of about 8 keV; structures arising from Auger-electron emission are superimposed on the continuum.

At the high-electron energies and at the forward angles, the broad peaked structure, the "binary-encounter peak" (BEP), due to electron emission following collisions with maximum momentum transfer, dominates the cross section. The BEP energy position is strongly dependent on the electron observation angle θ, and is given by $E(\mathrm{BEP})=4t\cos^2\theta$, where t is the projectile energy reduced by the ratio of the projectile to electron mass. The broad peaked electron distribution extending towards lower energies next to the BEP is the "electron-loss peak" (ELP). Its energy position is given by t; it is independent of the electron observation angle. The intensities of the BEP and ELP decrease with increasing observation angles. The angular dependence of the BEP causes an an-

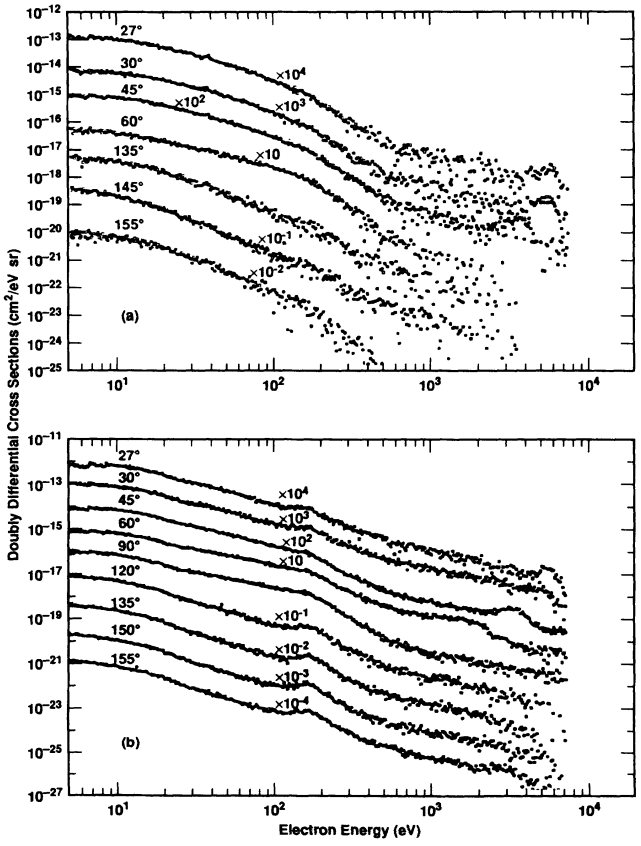

FIG. 1. Doubly differential cross sections for secondary-electron emission measured as a function of observation angles for 3.5-MeV/u Fe^{22+} colliding with (a) He and (b) Ar gas targets.

gular dependent overlap with the ELP which determines the shape of the electron energy distribution at higher electron energies. The doubly differential cross sections multiplied by the electron energy for forward angles are shown in Figs. 3(a) and 3(b) for the different projectile charge states and He and Ar targets. This particular plotting of the data makes some specific differences in the cross sections more visible. Since the intensities of the BEP and ELP vary with the projectile, the target, and the electron emission angle, it is expected that the shapes of the electron distribution at the energies, where the two peaks overlap, will deviate from one another and may lead to an interpretation as an interference pattern from continuum electrons centered at the projectile (ELP) and the target (BEP). However, for lower collision energies, coincidence measurements between electrons and projectile ions in specific charge states performed by Hagmann and collaborators [17], showed unexpected broad peaked energy distributions in the electron spectra. The angular dependence of this structure is inconsistent with that of

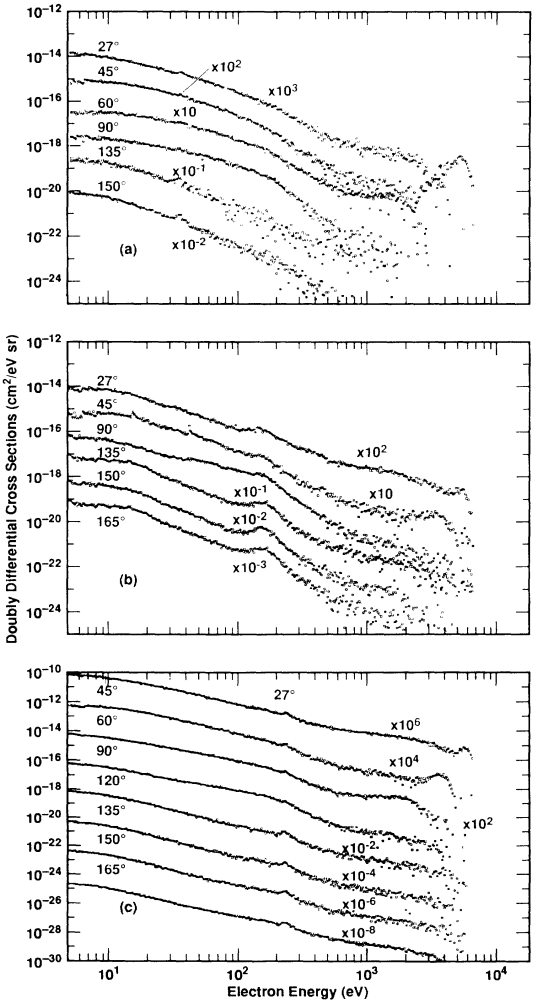

FIG. 2. Doubly differential cross sections for secondary-electron emission measured as a function of observation angles for 3.5-MeV/u Fe^{17+} colliding with (a) He, (b) Ar, and (c) CH_4 gas targets.

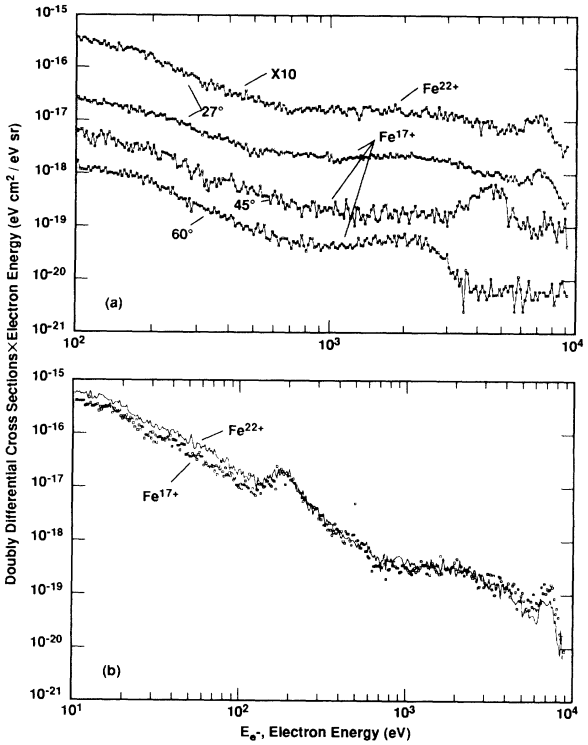

FIG. 3. Doubly differential cross sections multiplied by the electron energy are plotted vs the electron energies for $Fe^{17+,22+}$ incident on (a) He and (b) Ar gas targets.

the binary encounter or electron-loss peaks. The structure is attributed to a diffraction pattern of electrons which are elastically scattered off the screened projectile potential [18]. Figure 3(b) shows that, for the case of the Ar target, the cross sections are higher for Fe^{22+} than for Fe^{17+} at low electron energies up to about the Ar L Auger-electron structure in accordance to PWBA predictions. At higher electron energies the Fe^{17+} exceeds that of the Fe^{22+} and is about 40% larger at the BEP maximum. In the following we summarize our observations derived from a comparison of the measured doubly differential cross sections (DDCS's) for the different cases in Figs. 1 and 2.

For the case of 3.5-MeV/u Fe^{22+} on He and Ar the DDCS's for Ar are higher, in particular, towards higher electron energies, compared to the DDCS's for He. This is due to the ionization of electrons with much higher binding energies in Ar (wider velocity distributions). The intensity due to the ELP is weak. At backward angles, the intensity due to Ar K Auger-electron emission is observed for the case of Fe^{22+} on Ar.

For the case of 3.5-MeV/u Fe^{17+} on He, Ar, and CH_4 we observe that the DDCS's for Ar are the highest. The intensity for the ELP, however, is enhanced because of the larger number of electrons in the Fe^{17+} projectile ions as compared to Fe^{22+}. In addition, the BEP is enhanced in the case of the Fe^{17+} impact as compared to Fe^{22+} for the He target. This is believed to be an indication for contributions from projectile-electron–target-electron interaction affecting the production of the BEP [19]. The

target "active" electron (the one to be ionized) must interact with the projectile nucleus in a close collision, to be ejected in the BEP energy region. So this active electron must penetrate the cloud formed by the projectile electrons changing from the external weaker potential produced by the net projectile charge $q+$ to the inner stronger potential produced by the projectile nuclear charge Z_p. This change increases the slope of the projectile attractive potential with respect to a bare nucleus potential, increasing thus the ionization probability of the active electron before its collision with the projectile nucleus. Therefore the expected results would be an increase of the BEP as $q+$ decreases. This effect has also been observed in recent measurements of F^{q+} ions on H_2 and He targets [20] and of Cu^{q+} ions on He targets [21]. Measurements with heavier projectiles like U^{q+} (Ref. [22]) show interference effects in the BEP which have been related to interference structures in the elastic differential cross section for scattering of target electrons from the impinging ion. These are associated with the phenomenon of rainbow scattering [23].

Figure 4 shows our DDCS's measured at the most forward and backward angles in comparison with the experimental cross sections reported in Ref. [10] and scaled according to the Born approximation as Z_p^2/v^2 where v is the projectile ion velocity. The cross sections in Ref. [10] were measured for totally stripped C^{6+} ions. For the case of the He target the cross sections reported in Ref. [10] reached up to electron energies of 2–3 keV, for the Ar target up to 8 keV (at forward angles). The comparison with the scaled DDCS's shows the same behavior as reported previously: For the Fe^{22+} case the scaled DDCS's are lower at forward angles and higher at backward angles compared to our measured cross sections. A similar behavior is also observed for the Fe^{17+} case. In the present work the electron emissions were measured up to electron energies of 8 keV; this permits a comparison of our DDCS's with the scaled Ar results of Ref. [10] in the BEP region. It is observed that for the case of Ar at forward angles the agreement between the scaled and our measured DDCS's is good for the BEP region. However, no comparison is possible for the case of He in this energy region, since the measurements in Ref. [10] did not reach high enough in electron energy.

The angle and energy dependence of secondary-electron emission following fast heavy-ion-atom collisions has been well documented previously (see, e.g., Refs. [1,11]). However, recently new results and theoretical treatments have established additional effects in particular with respect to the angular dependence. This is demonstrated by a comparison with theoretical results using a quantum-mechanical treatment as carried out with the CDW-EIS. In these calculations Roothaan-Hartree-Fock bound-state wave functions, distorted by

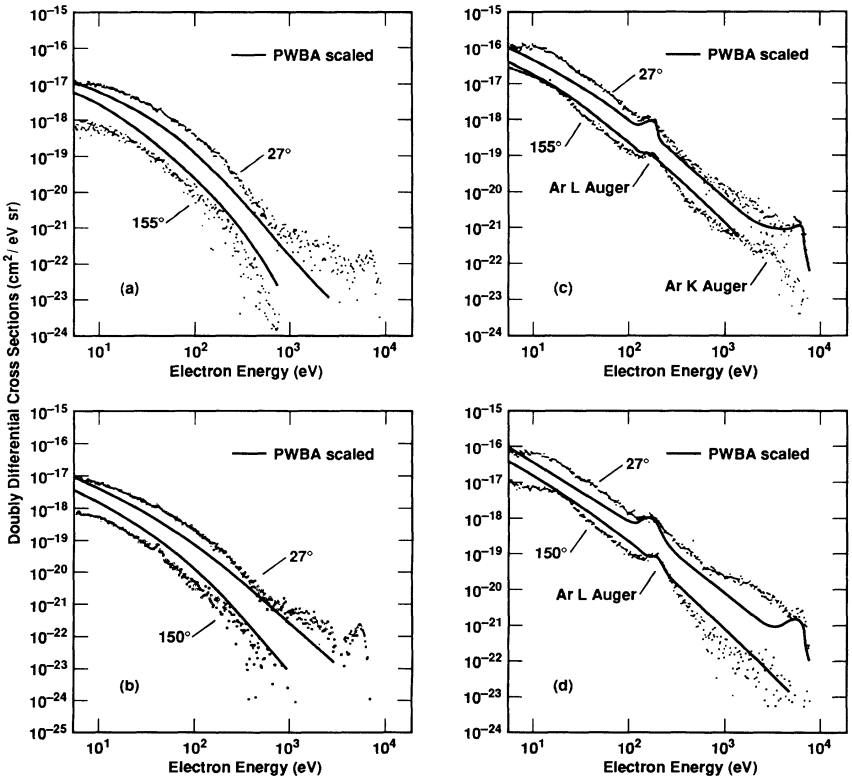

FIG. 4. Doubly differential cross sections measured for the most forward and backward angles from Figs. 1 and 2 [3.5-MeV/u Fe^{22+} colliding with (a) He and (c) Ar gas targets, 3.5-MeV/u Fe^{17+} colliding with (b) He and (d) Ar gas targets] compared with scaled cross sections from previous experiments [5-MeV/u C^{6+} on He and Ar targets (Ref. [10]). Scaling was carried out according to the PWBA.

an eikonal phase, have been used. The final state is represented as a product of continuum waves (Coulombic) centered at both the target and projectile, i.e., two Coulombic potentials are present in the final state (see Fainstein and Rivarola) [15]. Extended CDW-EIS calculations have been performed for the case of 3.5-MeV/u Fe^{22+} on He. In the entry channel an effective projectile charge $q+$ has been used in the eikonal phase, and in the exit channel effective charges $q+$ and $\xi_T=(-2\varepsilon_i)^{1/2}$ (with ε_i the Roothaan-Hartree-Fock initial orbital energy) have been employed in the projectile and target continuum factors, respectively. The comparison between experiment and theory is represented in Fig. 5 together with PWBA results. The PWBA calculations have been developed by Salin [23] by using an analytical potential which reproduces the Herman-Skillman potential [24] to describe the interaction between each active electron and the remnant He^+ core. The target bound initial and continuum final states are represented by Hartree-Fock-Slater functions. The following picture for the electron emission following highly charged heavy-ion collisions with atoms in single collisions may be inferred from a comparison with the theory.

At *low* electron energies the electron production could be expected to be dominated by the target ionization occurring at large impact parameters and the cross section would be described by a single-center emission picture treated in the Born approximation. However, important deviations from the PWBA predictions are obtained even at low electron energies, as can be seen for backward electrons. For *higher* electron energies the single-center emission concept was found to break down at forward and backward angles. These observations are attributed to higher-order effects. From the comparison with the CDW-EIS calculations we infer that for electron energies, ranging from a few eV up to a few keV, the two-center emission picture accounts for the experimental observations as shown and interpreted previously. It seems evident that at higher electron energies the outgoing electron is affected by the two-center system formed by the recoiling target and projectile ions. However, two-center effects are also observed at low electron energies due to the high charge of the projectile. At *very high* electron emission energies, at above 2 keV, it could be expected that the outgoing electron is affected by a single center consisting of both nuclei. This picture implies that the electron continuum reflects the effect of a varying Coulomb potential from the projectile and target nuclei. The electron emission spectrum is then determined by the dynamic change of the screening of the two nuclei and the outgoing electron. At higher impact velocities, the slow electrons are expected to sense only a single (target) emission center, the moderately fast electrons to sense two emission centers (target and projectile), and the very fast electrons again to sense both centers united to a single point.

The picture discussed here is also generally in agreement with the fact that the low-energy electrons are produced at large impact parameters, while the high-energy electrons are produced in small impact parameter collisions. The latter produce high-energy electrons which quickly escape the united atoms. In order to give an idea about the range of impact parameters, the electron energy scale in Fig. 5 has been converted into an approximate impact parameter scale, using the Massey criterion, to estimate the adiabatic radius R_{ad}. The comparison with the calculated cross sections in Fig. 5 shows strong disagreement with the PWBA results, particularly also in the BEP. On the other hand, the CDW-EIS calculations agree well with the measured results for forward angle emission, but disagree for the BEP. The CDW-EIS calculations tend to disagree also for higher electron ener-

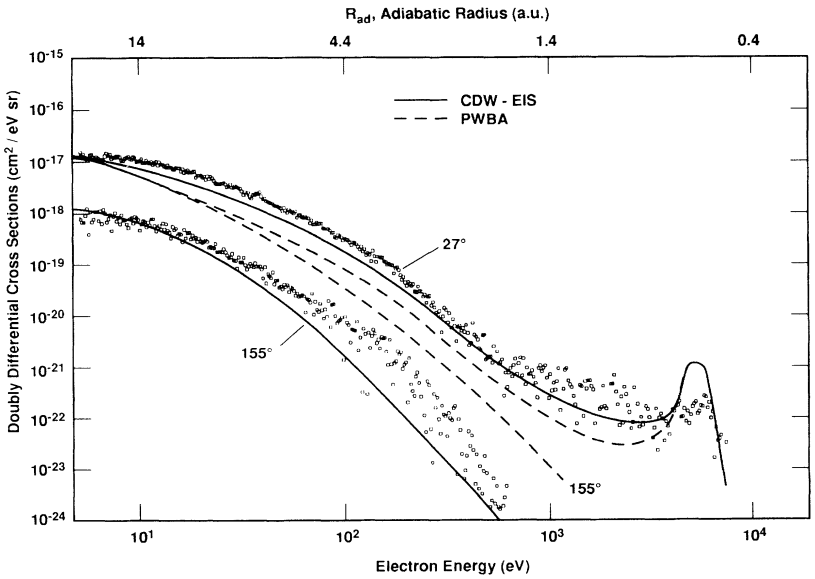

FIG. 5. Comparison of calculated cross sections [PWBA by Salin (Ref. [23]) and CDW–EIS] with experimental data for 3.5-MeV/u Fe^{22+} on He. Both the electron energy scale as well as the approximate impact parameter scale, using the Massey criterion, to estimate the adiabatic radius R_{ad} are given along the abscissa.

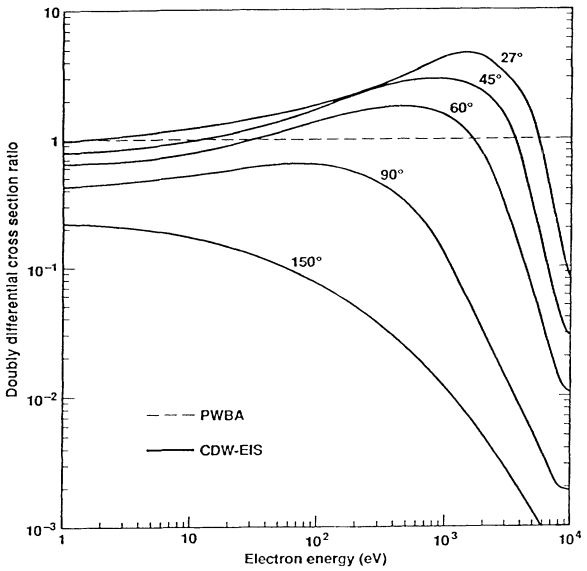

FIG. 6. Theoretical doubly differential cross section ratios from PWBA and CDW-EIS calculation for 3.5-MeV/u Fe^{22+} on He.

gies at the backward angle. The agreement over a wide range of electron energies, however, clearly favors the CDW-EIS calculations. The disagreement, in particular in the BEP region, is currently not clearly understood.

To further illustrate this disagreement, we present a comparison of the theoretical doubly differential cross section in Fig. 6. We plot the ratios of the doubly differential cross sections, as calculated by the CDW-EIS and the PWBA methods, for the case of 3.5-MeV/u Fe^{22+}. The ratios plotted are given by

$$\frac{1}{22^2}\frac{d\sigma_{\text{CDW-EIS}}(Z_p=22)}{dE\,d\Omega}\Big/\frac{d\sigma_{\text{PWBA}}(Z_p=1)}{dE\,d\Omega}\,.$$

The results of the CDW-EIS calculations show a significant deviation from these obtained with the PWBA. This deviation is observed to increase as one moves from intermediate angles (60°–90°) either to forward angles (45° and 27°) or to backward angles (150°). (A similar trend has also been observed above comparing the experimental DDCS'S with the PWBA results.) Specifically in the lower electron energy region (below 100 eV), the deviation from the PWBA increases with increasing angle. This effect arises because, for the system studied, the PWBA must overestimate the total- and single-differential $d\sigma/dE$ cross sections. It must be noted that comparing the DDCS is a more sensitive test than comparing the cross sections integrated over the solid angles. [When integrating the factor $\sin\theta$ makes preferable contributions at intermediate angles (near 90°) and smaller contributions at further forward and backward angles.] As expected, when the electron energy increases above 100 eV, two-center effects become more important which cause the CDW-EIS results to increase at forward and intermediate angles compared to the PWBA. At even larger energies (above 1 keV) a pronounced decrease of the ratio is observed for all angles [16]. As pointed out above, this effect is currently not clearly understood and needs further study.

CONCLUSION

Absolute doubly differential cross sections have been measured for electron emission in collisions of 3.5-MeV/u Fe^{17+} and Fe^{22+} ions incident on He, Ar, and CH_4 gas targets under single-collision conditions. The cross section have been compared to previous experimental cross section scaled according to the Born approximation. Strong deviations between calculated and scaled PWBA results (e.g., Fe^{22+} on He) and experimental cross sections were found. Good agreement was observed for the case of Fe^{22+} on He between experimental and theoretical doubly differential cross sections using CDW-EIS calculations except for the binary-encounter peak around 6-keV electron energy. To understand this deviation further theoretical and experimental investigations are necessary.

ACKNOWLEDGMENTS

The authors would like to acknowledge the support of the Lawrence Berkeley Laboratory SuperHILAC operations crew. They would like to thank Professor A. Salin for providing them with the unpublished PWBA results. One of the authors (R.D.R.) also would like to thank Professor A. Salin and Dr. V. H. Ponce for fruitful discussions. Two of the authors (P.F. and R.D.R.) received partial support from the International Atomic Energy Agency under Contract No. 5365/R1/RB. This work was performed under the auspices of the U.S. Department of Energy by the Lawrence Livermore National Laboratory under Contract No. W-7405-ENG-48.

[1] D. Schneider, D. DeWitt, A. S. Schlachter, R. E. Olson, W. G. Graham, J. R. Mowat, R. D. DuBois, D. H. Loyd, V. Montemayer, and G. Schiwietz, Phys. Rev. A **40**, 2971 (1989), and references quoted therein.

[2] M. E. Rudd and T. Jorgensen, Jr., Phys. Rev. **131**, 666 (1963); C. E. Kuyatt and T. Jorgensen, *ibid.* **130**, 144 (1963); M. E. Rudd, C. A. Sauter, and C. L. Bailey, *ibid.* **151**, 20 (1966).

[3] L. H. Toburen, Phys. Rev. A **3**, 216 (1971); L. H. Toburen and W. E. Wilson, *ibid.* **5**, 247 (1972).

[4] N. Stolterfoht, Z. Phys. **248**, 81 (1971).

[5] S. T. Manson, L. H. Toburen, D. H. Madison, and N. Stolterfoht, Phys. Rev. A **12**, 60 (1975); S. T. Manson (private communication).

[6] M. E. Rudd, L. H. Toburen, and N. Stolterfoht, At. Data Nucl. Data Tables **18**, 413 (1976).

[7] D. R. Gibson and I. D. Reid, J. Phys. B **19**, 3265 (1986).

[8] Y. K. Kim and M. Inokuti, Phys. Rev. A **12**, 1257 (1973).

[9] N. Stolterfoht, D. Schneider, D. Burch, H. Wiemann, and J. S. Risley, Phys. Rev. Lett. **33**, 59 (1974).

[10] H. Platten, Ph.D. thesis, Hahn-Meitner Institut, 1986 (unpublished); G. Schiwietz, H. Platten, D. Schneider, T.

Schneider, W. Zeitz, K. Musiol, R. Kowallik, and N. Stolterfoht, Hahn-Meitner Institut Report No. HMI-B447, Berlin, 1987.

[11] N. Stolterfoht, D. Schneider, J. Tanis, H. Altevogt, A. Salin, P. D. Fainstein, R. Rivarola, J. P. Grandin, J. H. Scheurer, S. Andriamonje, D. Bertault, and J. F. Chemin, Europhys. Lett. **4**, 899 (1987).

[12] G. Schiwietz and W. Fritsch, J. Phys. B **20**, 5463 (1987), and references quoted therein.

[13] R. E. Olson, in *Electronic and Atomic Collisions,* edited by Gilbody *et al.* (North-Holland, Amsterdam, 1987); R. E. Olson, J. Phys. B **12**, 1843 (1979).

[14] C. O. Reinhold and R. E. Olson (unpublished).

[15] P. D. Fainstein and R. D. Rivarola, J. Phys. B **20**, 1285 (1987); R. D. Rivarola and P. D. Fainstein, Nucl. Instrum. Methods B **24/25**, 240 (1987); P. D. Fainstein, V. H. Ponce, and R. D. Rivarola, J. Phys. B **21**, 287 (1988).

[16] P. D. Fainstein, V. H. Ponce, and R. D. Rivarola, J. Phys. (Paris) Colloq. **1**, C-183 (1989).

[17] S. Hagmann (private communication).

[18] C. Kelbch, S. Hagmann, S. Kelbch, R. Mann, R. E. Olson, S. Schmidt, and H. Schmidt-Böcking, Phys. Lett. A **139**, 304 (1989).

[19] R. E. Olson, C. O. Reinhold, and D. R. Schultz, J. Phys. B **23**, L456 (1990); C. O. Reinhold, D. R. Schultz, and R. E. Olson, *ibid.* **23**, L591 (1990).

[20] P. Richard, D. H. Lee, T. J. M. Zouros, J. M. Sanders, and J. L. Shinpaugh, J. Phys. B **23**, L213 (1990).

[21] O. Jagutzki, S. Hagmann, H. Schmidt-Böcking, D. R. Schultz, R. Dörner, R. Koch, A. Skutlartz, A. Gonzalez, C. Kelbch, and P. Richard, J. Phys. B **24**, 2579 (1991).

[22] C. O. Reinhold, D. R. Schultz, R. E. Olson, C. Kelbch, R. Koch, and H. Schmidt-Böcking, Phys. Rev. Lett. **66**, 1842 (1991).

[23] A. Salin (private communication).

[24] F. Herman and S. Skillman, *Atomic Structure Calculations* (Prentice-Hall, Englewood Cliffs, NJ, 1963).